

Facile preparation of Au(111)/MICA substrates for high-quality graphene nanoribbon synthesis

M. G. Hell^{*,1}, B. V. Senkovskiy¹, A. V. Fedorov¹, A. Nefedov², C. Wöll², A. Grüneis¹

¹ II. Physikalisches Institut, Universität zu Köln

² Institut für Funktionelle Grenzflächen, Karlsruher Institut für Technologie, Eggenstein-Leopoldshafen

Received XXXX, revised XXXX, accepted XXXX

Published online XXXX

Key words: Graphene nanoribbon, DBBA, Au(111), XPS, NEXAFS, Raman

* Corresponding author: e-mail hell@ph2.uni-koeln.de, Phone: +49 - 221 - 470 7078

A setup for the preparation of oriented Au(111)/mica thin films of ~ 100 nm thickness as an active substrate for graphene nanoribbon growth is shown. Low-energy electron diffraction shows that the Au(111) thin films have a single crystallographic orientation over the whole surface area. Graphene nanoribbons are synthesized by the bottom-up approach via surface polymerization of precursor molecules that are evaporated onto the catalytically active Au(111)/mica substrate. The graphene nanoribbons are investigated by a combination of resonance Raman, X-ray photoemission spectroscopy and near-edge X-ray

absorption fine structure spectroscopy confirming a nanoribbon quality equal to nanoribbons grown on commercially available single-crystal Au(111) substrates. The present work therefore establishes the in-situ preparation of Au(111)/MICA as an inexpensive and simple method to prepare substrates of desired shape and thickness for surface polymerization reactions which are of interest to a growing community of researchers working on graphene nanoribbons.

Copyright line will be provided by the publisher

1 Introduction Carbon nanomaterials have been in the focus of condensed matter physics for a long time already. Following fullerenes, nanotubes and graphene the latest member of this materials' family are graphene nanoribbons which are receiving lots of attention [1–4]. Ultranarrow graphene nanoribbons (GNRs) are ~ 1 nm wide stripes of graphene with defined edges (zig-zag or armchair). They can be produced in high-quality by bottom-up nanotechnology [2]. A large variety in structures can be engineered by simply varying the precursor molecule. Probably the best studied is the surface polymerization of 10,10-dibromo-9,9-bianthryl (DBBA) molecules which yields armchair graphene nanoribbons with a width of 7 atoms (7-AGNRs) [2, 5]. Modifications of the precursor molecule has successfully allowed for the bottom up synthesis of boron [6, 7] and sulphur doped nanoribbons [8]. Moreover, varying the width of the precursor

molecules changes the nanoribbon width and hence allows for band-gap engineering. For any of the precursors, surface polymerization can be obtained on atomically flat Au(111), Ag(111) or Cu(111) surfaces [2, 9, 10] (or their vicinal cuts such as Au(788) [11]). Single crystals have been used extensively for nanoribbon synthesis however their high cost is prohibitive for high-yield and scalable growth on an industrial scale. Nevertheless an atomically flat metal surface is needed to achieve reproducible and high-quality nanoribbon synthesis. The present manuscript addresses these needs. Here we show that the application of a well-known recipe for growth of Au(111) on muscovite mica [12] provides surfaces that can be synthesized in-situ and are inexpensive and easy-to-prepare.

2 Synthesis The Au(111)/MICA synthesis was performed in a small growth chamber under high vacuum

Copyright line will be provided by the publisher

conditions with the base pressure $p < 10^{-6}$ mbar. After Au(111) growth these substrates have been transferred in air into an ultra-high-vacuum (UHV) preparation chamber where the in-situ GNR synthesis and spectroscopy was performed. Prior to the GNR growth the Au(111) surfaces were gently annealed at 200°C to remove contaminants from the air exposure.

In figure 1(a) we show the core of the setup for preparation of Au(111)/MICA. It is a homebuilt sample manipulator which consists of a sample pocket, thermocouple and a water cooled quartz microbalance. Figure 1(b) depicts a sketch of how the sample plate (an Omicron type plate made out of Mo) can be inserted into the sample pocket. To prepare an Au(111) film we first mount a freshly ex-situ cleaved mica on the sample plate using Ta stripes, place into the sample pocket and evacuate it to a pressure lower than 10^{-6} mbar. We then clean and degas the sample by annealing to 300°C for at least 12 hours. Hereafter the mica is annealed to 500°C for ~ 1 min in order to remove contaminants. To obtain thick Au layer, the evaporator was placed close (about 5 cm) in front of the sample manipulator. The Au atom flux is calibrated conveniently just before deposition by a quartz microbalance and mounted above the sample pocket [see Figure 1(a)]. It is known [12] that for crystalline Au growth the mica must be kept at 300°C during deposition. We found that the Au deposition rate must be at least 0.5 \AA s^{-1} in order to obtain low energy electron diffraction (LEED) spots. After Au deposition the sample is annealed for 12 h at 300°C. Figure 1(c) depicts a photograph of an Au/mica film. Atomic force microscopy (AFM) enables precise thickness measurements and we have used AFM in order to calibrate the quartz microbalance tooling factor.

Figure 1(d) shows an atomic force microscopy (AFM) scan across the edge of the Au film. The edge was defined by the Ta stripe and therefore not perfectly sharp as some Au can grow underneath the stripe close to its edge. AFM allows to measure the thickness of the Au film which is defined by the height difference of the region under the Ta stripe to the maximum. An Au film prepared in such a way does not show a sharp pattern in low-energy electron diffraction (LEED). Hence such films are not ordered. In order to obtain a sharp LEED, a second annealing step at a temperature of 600°C is needed. This will cause the structuring of the Au(111) sample. The duration of the last annealing step is depending on the thickness of the sample. For a regular sample of 50-100 nm a duration of 30 minutes is sufficient. Hereafter we were able to identify a sharp LEED pattern with a sixfold rotational symmetry which we ascribe to the Au(111) surface structure. Two typical LEED patterns for electron energies of 50 and 70 eV taken prior to molecular deposition are shown in Figure 1(e), correspondingly. By scanning the sample across the LEED spot, we could verify that the LEED pattern does not change. This indicates that all domains have the same orientation in the topmost atom layers.

The synthesis of GNRs was performed by evaporation of DBBA molecules onto a freshly prepared Au(111) surface, followed by annealing steps. The DBBA was evaporated from a quartz crucible using a homebuilt organics evaporator with a thermocouple attached to the molecule reservoir. The deposition rate was controlled using a quartz microbalance. About 10 \AA of precursor molecules (using the graphite density and Z-factor) were evaporated onto the Au surface which was kept at room-temperature. Effectively only a part of the DBBA will form ribbons and the remainder will simply sublime. This is due to a weaker bonding between molecules to each other with respect to the molecule-substrate bond. In order to carry out DBBA debromization and cyclodehydrogenation reactions, the temperatures must be known quite precisely (to an accuracy better than 5°C) and annealing has to be carried out slowly. We have therefore calibrated this curve not with the thermocouple shown in Figure 2(a), instead we have spot-welded a thermocouple onto an empty sample holder and recorded the temperature directly where usually the mica is located. Figure 2(a) shows the curve of temperature versus time we have used to synthesize graphene nanoribbons from a 10 \AA thick DBBA film/Au(111)/mica. The inset to Figure 2(a) depicts a sketch of the DBBA molecule.

3 Results The straightforward way to proof the formation of GNRs is resonance Raman spectroscopy. GNRs have a radial-breathing like mode at low energies (397 cm^{-1}) for 7-AGNR [13]) which is their fingerprint. Due to the high resonance enhancement that occurs if the laser energy used matches the separation of van-Hove-singularities in the density of electronic states, very strong Raman spectra from submonolayer coverages of ribbons can be obtained easily. The E_{22} resonance transition for 7-AGNRs can be excited by a 2.35 eV laser [14]. Figure 2(b) depicts the Raman spectra obtained. It can be seen that all GNR related modes appear. In particular, the defect induced D band is even lower than of most GNRs synthesized on single crystal substrates. [2]

Then we turn to the x-ray photoemission spectroscopy (XPS) measurements on C and Br core levels which have been carried out at the HESGM beamline of the BESSY II synchrotron (Helmholtz-Zentrum Berlin, Germany). Figures 2(c) and 2(d) depict the C1s and Br3d core levels during three annealing steps (room temperature, 200°C and 400°C). The photon energy used was set to $h\nu=385 \text{ eV}$. It can be seen that the intensity for C1s is not changing during polymerization and a lot of the Br3d intensity vanishes after the first annealing step of 200°C. Further annealing to 400°C causes all Br3d intensity to disappear, indicating that the Br has left the Au surface and that all the molecules are now either in their radical form with dangling C atoms or already polymerized.

After that near edge x-ray absorption fine structure (NEXAFS) spectroscopy have been performed in partial yield mode. Figure 2(e) depicts the C K-edge NEXAFS

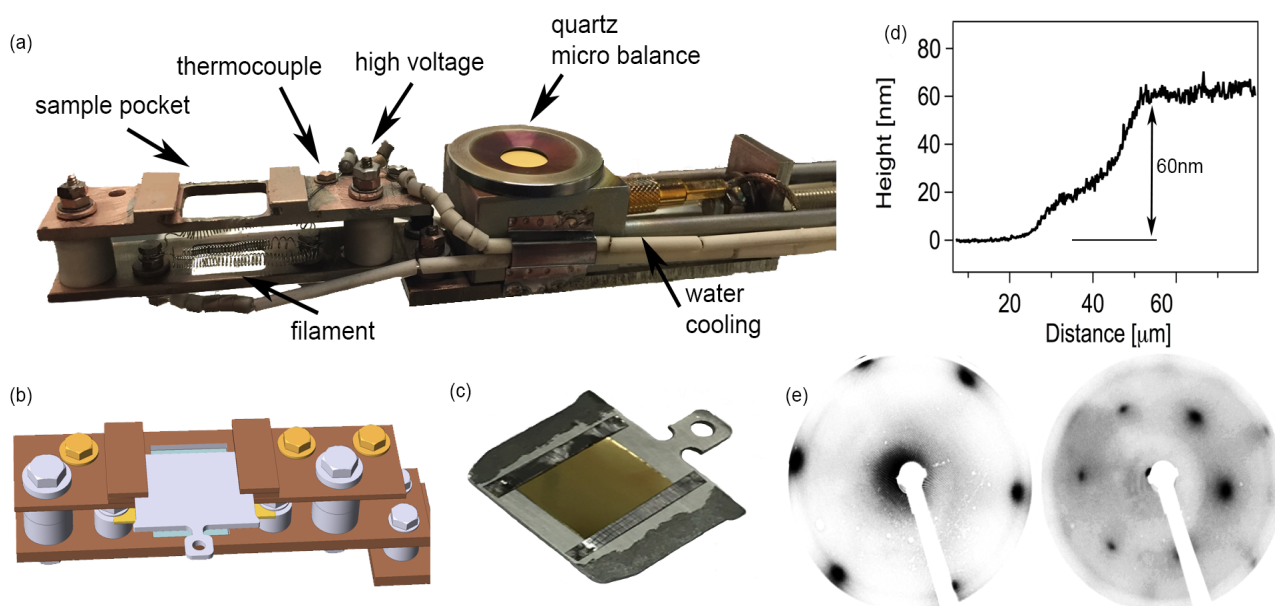


Figure 1 (a) Homebuilt sample manipulator with empty sample pocket, filament and high voltage for e-beam heating, thermocouple and water cooled quartz microbalance (b) schematics of a sample inserted into the sample pocket (c) MICA after deposition of Au (d) AFM measurement of Au(111) height on MICA across the location of the Ta stripe (e) LEED diffraction pattern of Au(111)/mica at 50 eV and at 70 eV.

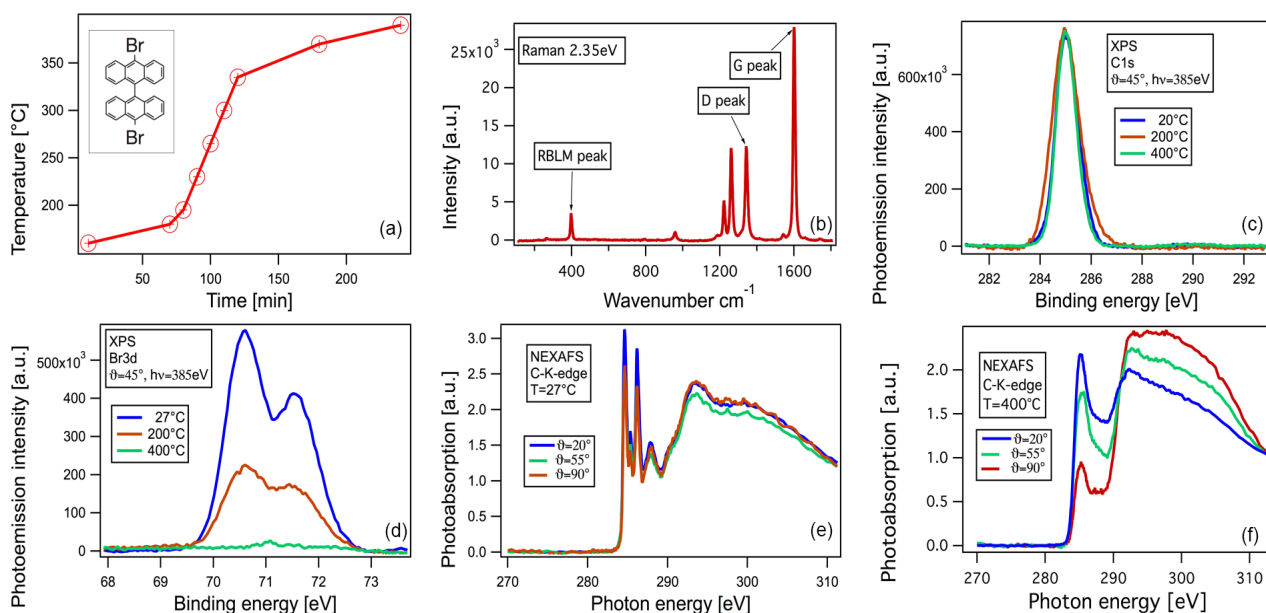


Figure 2 (a) Temperature programmed GNR synthesis performed with a programmable power supply (b) Raman spectrum of 7-AGNRs on Au(111) measured with a 2.35 eV laser (c,d) XPS spectra of C1s and Br3d core levels (e,f) NEXAFS spectra of deposited DBBA molecules immediately after deposition and after annealing to 400°C.

spectra measured at three different incidence angles on DBBA molecules deposited on Au before annealing. The sharp features at the photon energy range 284-290 eV are related to transitions from the C1s core levels to the un-

occupied π^* molecular orbitals. Since a significant angle dependence is absent we can conclude that the precursor molecules are disordered or partially twisted with a small tendency to planar orientation. After annealing up

to 400°C a drastic change in the electronic structure takes place. The corresponding NEXAFS spectra are shown in Figure 2(f). Firstly, the sharp peaks in the π^* resonance at 285 eV disappear and a rather broad peak appears. Secondly, the angle dependence of this new peak as well as of σ^* resonances now much stronger. In particular the π^* related peak around 285 eV has a minimum and σ^* related peaks at the photon energy range 290-310 eV have a maximum for normal incidence (90°, the electric field vector is parallel to the ribbon plane). This angle dependence indicates that the GNRs are lying planar on the surface after cyclodehydrogenation.

4 Conclusions In summary we have shown an inexpensive and simple method to prepare high quality disposable Au(111)/MICA substrates for the surface polymerization of graphene nanoribbons using a molecular precursor. The spectroscopic investigation of GNR samples grown on this substrate indicates that the GNRs have spectra identical to those obtained from single crystal substrates. This has been checked using Raman spectroscopy, XPS and NEXAFS. The Au(111)/mica substrates are much cheaper than the single crystals, and, thus, can be used for experiments, that are harmful for substrates (e.g. chemical treatment and functionalization or transferring the GNRs on to the insulators/semiconductors). The method introduced here is important for the growing GNRs community which wishes to synthesize GNRs on purpose made substrates.

Acknowledgements M.H., B.S. and A.G. acknowledge the ERC grant no. 648589 'SUPER-2D', funding from Quantum Matter and Materials and DFG project GR 3708/2 – 1. A.N. and C.W. acknowledge funding from the Science and Technology of Nanosystems program. Research supported by the U.S. Department of Energy (DOE), Office of Science, Basic Energy Sciences (BES), under Award no. *DE – SC0010409* (design, synthesis and characterization of molecular building blocks) and the Center for Energy Efficient Electronics Science NSF Award 0939514 (SPM imaging and spectroscopy). We also thank Helmholtz Zentrum Berlin for the beamtime allocation.

References

- [1] L. Grill, M. Dyer, L. Lafferentz, M. Persson, M. V. Peters, and S. Hecht, *Nature Nanotechnology* **2**, 687–691 (2007).
- [2] J. Cai, P. Ruffieux, R. Jaafar, M. Bieri, T. Braun, S. Blankenburg, M. Muoth, A. P. Seitsonen, M. Saleh, X. Feng, K. Mullen, and R. Fasel, *Nature* **466**(7305), 470–473 (2010).
- [3] Z. Chen, Y. M. Lin, M. J. Rooks, and P. Avouris, *Physica E: Low-dimensional Systems and Nanostructures* **40**(2), 228 – 232 (2007), International Symposium on Nanometer-Scale Quantum Physics.
- [4] P. Ruffieux, J. Cai, N. C. Plumb, L. Patthey, D. Prezzi, A. Ferretti, E. Molinari, X. Feng, K. Müllen, C. A. Pignedoli, and R. Fasel, *ACS Nano* **6**(8), 6930–6935 (2012).
- [5] A. Narita, X. Feng, and K. Müllen, *The Chemical Record* **15**(1), 295–309 (2014).
- [6] S. Kawai, S. Saito, S. Osumi, S. Yamaguchi, A. S. Foster, P. Spijker, and E. Meyer, *Nat Commun* **6**, 8098 (2015).
- [7] R. R. Cloke, T. Marangoni, G. D. Nguyen, T. Joshi, D. J. Rizzo, C. Bronner, T. Cao, S. G. Louie, M. F. Crommie, and F. R. Fischer, *Journal of the American Chemical Society* **137**(28), 8872–8875 (2015), PMID: 26153349.
- [8] G. D. Nguyen, F. M. Toma, T. Cao, Z. Pedramrazi, C. Chen, D. J. Rizzo, T. Joshi, C. Bronner, Y. C. Chen, M. Favaro, S. G. Louie, F. R. Fischer, and M. F. Crommie, *The Journal of Physical Chemistry C* **120**(5), 2684–2687 (2016).
- [9] K. A. Simonov, N. A. Vinogradov, A. S. Vinogradov, A. V. Generalov, E. M. Zagrebina, N. Mårtensson, A. A. Cafolla, T. Carpy, J. P. Cunniffe, and A. B. Preobrajenski, Growth and structure of graphene nanoribbons on substrates with different reactivity, www.maxlab.se.
- [10] K. A. Simonov, N. A. Vinogradov, A. S. Vinogradov, A. V. Generalov, E. M. Zagrebina, G. I. Svirskiy, A. A. Cafolla, T. Carpy, J. P. Cunniffe, T. Taketsugu, A. Lyalin, N. Mårtensson, and A. B. Preobrajenski, *ACS Nano* **9**(9), 8997–9011 (2015).
- [11] S. Linden, D. Zhong, A. Timmer, N. Aghdassi, J. H. Franke, H. Zhang, X. Feng, K. Müllen, H. Fuchs, L. Chi, and H. Zacharias, *Phys. Rev. Lett.* **108**(21) (2012).
- [12] R. Colton, W. Ebeling, J. Frommer, H. Gaub, A. Gewirth, R. Guckenberger, and J. Rabe, Wiley; 1 edition **ISBN-13: 978-0471959120** (August 7, 1998).
- [13] L. Talirz, P. Ruffieux, and R. Fasel, *Adv. Mater.*(feb), n/a–n/a (2016).
- [14] F. Krakau, Bachelor thesis, University of Cologne (2014).